Application of the Korringa-Kohn-Rostoker cluster coherent-potential approximation to an s phase shift semicircular model

1990 J. Phys.: Condens. Matter 2 2653

(http://iopscience.iop.org/0953-8984/2/11/010)

J. Phys.: Condens. Matter 2 (1990) 2653–2670. Printed in the UK

Application of the Korringa–Kohn–Rostoker cluster coherent-potential approximation to an s phase shift semicircular model

S S Rajput, S S A Razee, R Prasad and A Mookerjee†
Department of Physics, Indian Institute of Technology, Kanpur – 208016, India

Received 24 April 1989

Abstract. An s phase shift semicircular model of a random substitutional binary alloy has been used as a test case for studying the self-consistent Korringa–Kohn–Rostoker cluster coherent-potential approximation (KKR-CCPA). In addition to being computationally simpler, the model has the advantage that a corresponding model exists in the well known tight-binding framework. A one-to-one correspondence has been shown between the KKR-CCPA equations and the tight-binding CCPA equations. In the tight-binding framework, it has been shown that certain quantities, which were hitherto calculated approximately, can be obtained exactly by the partitioning technique. Our results for density of states in the CCPA show rich structure in the impurity band, which arises due to correlated scattering from clusters of atoms.

1. Introduction

During the last decade, the coherent-potential approximation (CPA) has emerged as the most successful single-site approximation for calculating the electronic structure of random substitutional binary alloys, in both the empirical tight-binding (TB) and first-principles Korringa–Kohn–Rostoker (KKR) frameworks. Despite its success, the CPA, being a single-site approximation, does not include correlated scattering from neighbouring sites. This could play an important role in systems having short-range order and clustering tendencies (Wright *et al* 1987, Stefanou *et al* 1987, Banhart *et al* 1988). To study the effect of correlated scattering, some workers (Gonis *et al* 1984) proposed the idea of an embedded cluster method. In this method, a cluster consisting of a central site and its shell of nearest neighbours was embedded in an effective medium determined within the KKR-CPA. However, this method is not fully self-consistent. The idea of self-consistent cluster CPA (CCPA) was proposed by some workers within the framework of some new approaches, like travelling-cluster approximation (Mills and Ratanavararaksa 1978) and augmented-space formalism (ASF) (Mookerjee 1973, Gray and Kaplan 1976a, b), which preserve the *herglotz* properties of the Green function. The ASF has been successfully applied to the calculation of electronic properties of binary alloys by several workers in the tight-binding framework (Kumar *et al* 1982, Thakur *et al* 1987).

Recently it has been shown that one can use the ASF to go beyond the single-site approximation within the conventional KKR method (Mookerjee 1987, Razee *et al* 1990), preserving the *herglotz* properties of the Green function. Because of its complexity,

† Present address: S N Bose National Centre for Basic Sciences, DB-17, Sector I, Salt Lake City, Calcutta 700064, India.

0953-8984/90/112653 + 18 $03.50

implementation of the KKR-CCPA to realistic systems is difficult and involves lengthy computation. To our knowledge no successful implementation has been carried out on any realistic system to date. In this paper, as a test case, we have applied the KKR-CCPA to an s phase shift semicircular model. The model has several advantages. (i) Because of the semicircular modelling, the involved $\boldsymbol{k}$-space integration, required to obtain the site-diagonal path operator, is bypassed. This reduces the computational effort and allows us to concentrate more on the effect of correlated scattering, which is the principal aim of this work. (ii) The KKR-CPA based on this model has been tried out before (Soven 1970). This allows us to compare the earlier work, based on conventional methods, with our augmented-space generalisation. However, the *ad hoc* assumption of a semicircular density of states for the structure factor allows us only to obtain the site-diagonal path operator. It does not tell us how to obtain the off-diagonal elements, which are also necessary in the CCPA. In order to circumvent this difficulty, we have first shown an *exact analogy* in the mathematical structure in the CCPA equations of the KKR method in this model and the tight-binding equations. The path operator in the KKR method has its counterpart in the Green function in the tight-binding framework. We have also shown, through the analogy, that the semicircular model is essentially a Bethe lattice approximation. This allows us to model the off-diagonal elements of the path operator. It also gives us a clear insight into the approximations involved in the model.

In section 2.1, we start with a brief discussion of the augmented-space formulation. This is first applied to a tight-binding Hamiltonian and CCPA equations are derived. This then forms the basis for extension of this method to the KKR framework. In the tight-binding framework, we have refined the technique such that various quantities appearing in the CCPA equations are calculated *exactly*. Till now these quantities were calculated approximately by summing over an infinite series (Kumar *et al* 1982, Thakur *et al* 1987).

One of the features of the CPA is that in the low-concentration limit it gives the features of a single impurity (Ehrenreich and Schwartz 1976). In the same spirit, we want to examine whether the CCPA density of states (DOS) in the low-concentration limit reduces to the two-impurity local density of states (LDOS). The formulation of the two-impurity problem is given in section 2.2. In some earlier work on the CCPA (Thakur *et al* 1987, Kumar *et al* 1982) as well as in the present work, we note rich structure in the CCPA DOS. We also wish to understand the structure in the CCPA DOS in the light of the two-impurity LDOS.

The formulation of the KKR-CCPA is presented in section 2.3. In section 3.1, we apply the KKR-CCPA formulation to the s phase shift semicircular model. The Bethe lattice model is examined in section 3.2. The KKR-CCPA equations for the s phase shift model and the tight-binding CCPA equations for the semicircular model are compared and a one-to-one correspondence between them is established in section 3.3. Finally we present our results in section 4 and our conclusions in section 5.

2. Formulation

2.1. Tight-binding cluster coherent-potential approximation (TB-CCPA)

We consider the following tight-binding Hamiltonian with no off-diagonal disorder:

$$H = \sum_i E_i \mathcal{P}_i + \sum_{i \neq j} \sum V_{ij} \mathcal{T}_{ij} \tag{2.1a}$$

where E_i is the energy corresponding to site i, and V_{ij} is the hopping integral. $\mathcal{P}_i$ $(=|i\rangle\langle i|)$

and $\mathcal{T}_{ij}$ ($=|i\rangle\langle j|$) are respectively projection and transfer operators in the Hilbert space $\mathcal{H}$ spanned by the site-labelled basis $\{|i\rangle\}$. The elements of the Green function for this system are

$$G_{ij} = \langle i|(EI - H)^{-1}|j\rangle. \tag{2.1b}$$

For a random binary alloy A_xB_y, the random site energy E_i can be written in terms of a random 'occupation' parameter n_i as

$$E_i = E_A n_i + E_B(1 - n_i) \tag{2.1c}$$

where

$$n_i = \begin{cases} 1 & \text{if } i = A \\ 0 & \text{if } i = B \end{cases}$$

with a probability distribution

$$p(n_i) = x\delta(n_i - 1) + y\delta(n_i).$$

We may express $p(n_i)$ as

$$p(n_i) = -(1/\pi)\,\mathrm{Im}\langle f_i^0|(n_i I - M_i)^{-1}|f_i^0\rangle$$

where M_i is an operator in the configuration space θ_i of rank 2 spanned by $|f_i^0\rangle$ and $|f_i^1\rangle$ with a representation

$$M_i = x\mathcal{P}_{f_i^0} + y\mathcal{P}_{f_i^1} + (xy)^{1/2}(\mathcal{T}_{f_i^0 f_i^0} + \mathcal{T}_{f_i^1 f_i^0}). \tag{2.2}$$

The augmented-space theorem (Mookerjee 1973) then implies that the configuration average of a function is

$$\langle f[\{n_i\}]\rangle = \langle\varphi|\,\tilde{f}[\{M_i\}]|\varphi\rangle \tag{2.3}$$

where $|\varphi\rangle = \Pi_i|f_i^0\rangle$ is a member of the basis $|\varphi_p\rangle = \Pi_i\,|f_i^{s_i}\rangle$ ($s_i = 0$, 1 and $p = 1, 2, \ldots, 2^N$) belonging to the configuration space $\Phi = \Pi_i\theta_i$ of rank 2^N. The function $\tilde{f}[\{M_i\}]$ is an operator in the augmented space $\psi = \mathcal{H} \otimes \Phi$ of rank $N \times 2^N$.

The elements of the configuration-averaged Green function, by the augmented-space theorem, are

$$\langle G_{ij}(E)\rangle = \langle i, \varphi|(EI - \tilde{H})^{-1}|\varphi, j\rangle. \tag{2.4a}$$

The augmented-space Hamiltonian $\tilde{H}$ is given by

$$\tilde{H} = E_B \otimes \mathcal{I} + \delta E \sum_i \mathcal{P}_i \otimes M_i + \sum\sum_{i \neq j} V_{ij}\mathcal{T}_{ij} \otimes \mathcal{I} \tag{2.4b}$$

where $\delta E = E_A - E_B$ and $\mathcal{I}$ is the identity operator in the configuration space. Note that (2.4*a*) is exact, but cannot be evaluated because of the large dimensionality of the augmented space. Therefore, we look for some approximation that will reduce the size of the augmented space. For this purpose, we partition the augmented space into a subspace I spanned by $|\mathcal{C}, \varphi_p\rangle$ and remaining subspace denoted by II. We shall take, as an example, the cluster $\mathcal{C}$ consisting of sites 0 and 1.

The subspace I is spanned by eight basis vectors $|0, \varphi\rangle$, $|0, \varphi_0\rangle$, $|0, \varphi_1\rangle$, $|0, \varphi_{01}\rangle$, $|1, \varphi\rangle$, $|1, \varphi_0\rangle$, $|1, \varphi_1\rangle$ and $|1, \varphi_{01}\rangle$, where $\varphi = |f_0^0 f_1^0\rangle$, $\varphi_1 = |f_0^0 f_1^1\rangle$, $\varphi_0 = |f_0^1 f_1^0\rangle$ and $\varphi_{01} = |f_0^1 f_1^1\rangle$ (Mookerjee 1973).

Now we partition $\tilde{H}$ as

$$\tilde{H} = \begin{pmatrix} H_{\mathrm{I}} & H' \\ H'^{\mathrm{T}} & H_{\mathrm{II}} \end{pmatrix}$$

where

$$\begin{aligned} H_{\mathrm{I}} = {} & \bar{E}[\mathcal{P}_0 \otimes (\mathcal{P}_{\varphi} + \mathcal{P}_{\varphi_1}) + \mathcal{P}_1 \otimes (\mathcal{P}_{\varphi_0} + \mathcal{P}_{\varphi})] \\ & + \hat{E}[\mathcal{P}_1 \otimes (\mathcal{P}_{\varphi_1} + \mathcal{P}_{\varphi_{01}}) + \mathcal{P}_0 \otimes (\mathcal{P}_{\varphi_{01}} + \mathcal{P}_{\varphi_0})] \\ & + (V_{01}\mathcal{T}_{01} + V_{10}\mathcal{T}_{10}) \otimes (\mathcal{P}_{\varphi} + \mathcal{P}_{\varphi_{01}} + \mathcal{P}_{\varphi_0} + \mathcal{P}_{\varphi_1}) \\ & + W[\mathcal{P}_0 \otimes (\mathcal{T}_{\varphi_1\varphi_{01}} + \mathcal{T}_{\varphi_{01}\varphi_1} + \mathcal{T}_{\varphi_0\varphi} + \mathcal{T}_{\varphi\varphi_0})] \\ & + W[\mathcal{P}_1 \otimes (\mathcal{T}_{\varphi\varphi_1} + \mathcal{T}_{\varphi_1\varphi} + \mathcal{T}_{\varphi_{01}\varphi_0} + \mathcal{T}_{\varphi_0\varphi_{01}})]. \end{aligned} \tag{2.5a}$$

We now replace the Hamiltonians H_{II} and H' by translationally symmetric effective Hamiltonians $H_{\mathrm{II}}^{\mathrm{eff}}$ and H'^{eff}. Their diagonal and off-diagonal elements are σ_0 and σ_{ij} respectively. Thus

$$\begin{aligned} H_{\mathrm{II}} &= \left(\sigma_0 \sum_{i\neq 0,1} \mathcal{P}_i + \sum\sum_{i,j\neq 0,1} \sigma_{ij}\mathcal{T}_{ij}\right) \otimes (\mathcal{P}_{\varphi} + \mathcal{P}_{\varphi_0} + \mathcal{P}_{\varphi_1} + \mathcal{P}_{\varphi_{01}}) \\ H' &= \left(\sum\sum_{i,j\neq 0,1} \sigma_{ij}\mathcal{T}_{ij}\right) \otimes (\mathcal{P}_{\varphi} + \mathcal{P}_{\varphi_0} + \mathcal{P}_{\varphi_1} + \mathcal{P}_{\varphi_{01}}) \end{aligned} \tag{2.5b}$$

$$\bar{E} = xE_{\mathrm{A}} + yE_{\mathrm{B}} \qquad \hat{E} = xE_{\mathrm{B}} + yE_{\mathrm{A}} \qquad W = (xy)^{1/2}(E_{\mathrm{A}} - E_{\mathrm{B}}).$$

By the partition theorem, $\langle G_{ij}\rangle$ may be written as the representation of the resolvent of an operator $\hat{H}$ in the subspace I where

$$\hat{H} = H_{\mathrm{I}} + H'(E\mathcal{I} - H_{\mathrm{II}})^{-1}H'^{\mathrm{T}}.$$

With the help of equations (2.5), we get

$$\hat{H} = H_{\mathrm{I}} + [\xi_{00}(\mathcal{P}_0 + \mathcal{P}_1) + (\xi_{01}\mathcal{T}_{01} + \xi_{10}\mathcal{T}_{10})] \otimes (\mathcal{P}_{\varphi} + \mathcal{P}_{\varphi_0} + \mathcal{P}_{\varphi_1} + \mathcal{P}_{\varphi_{01}})$$

where

$$\begin{aligned} \xi_{00} &= \sum\sum_{j,k\neq 0,1} \sigma_{0j} G_{jk}^{\mathrm{eff}(0,1)} \sigma_{k0} \\ \xi_{01} &= \sum\sum_{j,k\neq 0,1} \sigma_{0j} G_{jk}^{\mathrm{eff}(0,1)} \sigma_{k1} \\ \xi_{10} &= \sum\sum_{j,k\neq 0,1} \sigma_{1j} G_{jk}^{\mathrm{eff}(0,1)} \sigma_{k0}. \end{aligned} \tag{2.6}$$

Since we need only the $\langle i, \varphi| \ldots |\varphi, j\rangle$ element of $(E\mathcal{I} - \hat{H})^{-1}$, we again partition $\hat{H}$ as

$$\hat{H} = \begin{bmatrix} H_1 & H_{12} \\ H_{12}^{\mathrm{T}} & H_2 \end{bmatrix}$$

where

$$H_1 = \begin{pmatrix} \bar{E} + \xi_{00} & V_{01} + \xi_{01} \\ V_{10} + \xi_{10} & \bar{E} + \xi_{00} \end{pmatrix}$$

$$H_{12} = \begin{pmatrix} 0 & 0 & 0 & 0 & 0 & W \\ W & 0 & 0 & 0 & 0 & 0 \end{pmatrix}. \tag{2.7a}$$

The matrix H_2 is of rank 6 and can be obtained from equations (2.6). By the partition theorem

$$\langle i, \varphi|(E\mathcal{I} - \hat{H})^{-1}|\varphi, j\rangle = \langle i|[E\mathcal{I} - H_1 - H_{12}(E\mathcal{I} - H_2)^{-1}H_{21}]^{-1}|j\rangle. \tag{2.7b}$$

Here

$$H_{12}(E\mathcal{I} - H_2)^{-1}H_{21} = \begin{pmatrix} WQ_{66}W & WQ_{61}W \\ WQ_{16}W & WQ_{11}W \end{pmatrix}$$

where

$$Q_{ij} = [(E\mathcal{I} - H_2)^{-1}]_{ij}.$$

We define a translationally symmetric effective Hamiltonian H^{eff} such that its resolvent is the average Green function $\langle G_{ij}\rangle$:

$$H^{\text{eff}} = \sigma_0 \sum_i \mathcal{P}_i + \sum_{i \neq j}\sum \sigma_{ij}\mathcal{T}_{ij}. \tag{2.8}$$

Here σ_0 and σ_{ij} are diagonal and off-diagonal elements of H^{eff}. By comparing (2.7*b*) and (2.8), we get

$$\begin{aligned} \sigma_0 &= \bar{E} + WQ_{66}W \\ \sigma_{01} &= V_{01} + WQ_{61}W \\ \sigma_{10} &= V_{10} + WQ_{16}W. \end{aligned} \tag{2.9}$$

Here

$$\begin{aligned} Q_{66} &= R_6^{-1} \\ Q_{16} &= R_1^{-1}\mathcal{V}_{10}R_2^{-1}WR_3^{-1}\mathcal{V}_{01}R_4^{-1}WR_5^{-1}\mathcal{V}_{10}R_6^{-1} \\ Q_{61} &= R_\sigma^{-1}\mathcal{V}_{01}R_5^{-1}WR_4^{-1}\mathcal{V}_{10}R_3^{-1}WR_2^{-1}\mathcal{V}_{01}R_1^{-1}. \end{aligned} \tag{2.10}$$

with

$$\begin{aligned} \mathcal{V}_{01} &= V_{01} + \xi_{01} \\ \mathcal{V}_{10} &= V_{10} + \xi_{10} \end{aligned}$$

and

$$\begin{aligned} R_1 &= E - \bar{E} - \xi_{00} \\ R_2 &= E - \bar{E} - \xi_{00} - \mathcal{V}_{01}R_1^{-1}\mathcal{V}_{10} \\ R_3 &= E - \bar{E} - \xi_{00} - WR_2^{-1}W \\ R_4 &= E - \bar{E} - \xi_{00} - \mathcal{V}_{10}R_3^{-1}\mathcal{V}_{01} \\ R_5 &= E - \bar{E} - \xi_{00} - WR_4^{-1}W \\ R_6 &= E - \bar{E} - \xi_{00} - \mathcal{V}_{01}R_5^{-1}\mathcal{V}_{10}. \end{aligned} \tag{2.11}$$

We have calculated ξ_{00}, ξ_{01} and ξ_{10} analytically by using the partition theorem on H^{eff}. The G^{eff} is given as

$$G^{\text{eff}} = (EI - H^{\text{eff}})^{-1}.$$

By partitioning this in 2×2 cluster subspace, we get

$$\begin{pmatrix} G_{00}^{\text{eff}} & G_{01}^{\text{eff}} \\ G_{10}^{\text{eff}} & G_{00}^{\text{eff}} \end{pmatrix} = \left[\begin{pmatrix} E - \sigma_0 & -\sigma_{01} \\ -\sigma_{10} & E - \sigma_0 \end{pmatrix} - \begin{pmatrix} \xi_{00} & \xi_{01} \\ \xi_{10} & \xi_{00} \end{pmatrix} \right]^{-1}. \tag{2.12}$$

Equation (2.12) then gives

$$\begin{aligned} \xi_{00} &= E - \sigma_0 - [G_{00}^{\text{eff}} - G_{01}^{\text{eff}}(G_{00}^{\text{eff}})^{-1} G_{10}^{\text{eff}}]^{-1} \\ \xi_{01} &= -\sigma_{01} + [G_{00}^{\text{eff}} - G_{01}^{\text{eff}}(G_{00}^{\text{eff}})^{-1} G_{10}^{\text{eff}}]^{-1} G_{01}^{\text{eff}}(G_{00}^{\text{eff}})^{-1} \\ \xi_{10} &= -\sigma_{10} + (G_{00}^{\text{eff}})^{-1} G_{10}^{\text{eff}}[G_{00}^{\text{eff}} - G_{01}^{\text{eff}}(G_{00}^{\text{eff}})^{-1} G_{10}^{\text{eff}}]^{-1}. \end{aligned} \tag{2.13}$$

Note that ξ_{00}, ξ_{01} and ξ_{10} as given by (2.13) are exact. Earlier workers (Kumar *et al* 1982, Thakur *et al* 1987) calculated these quantities approximately from (2.6) by a recursion method.

2.2. *The two-impurity problem*

The study of the two-impurity problem is important while examining the structures in CCPA DOS. Let us embed two impurities A and B at the sites labelled as 0 and 1 in the CPA effective medium. Then the Hamiltonian is

$$H = \sigma_0 \sum_{i \neq 0,1} \mathcal{P}_i + \sum\sum_{i,j \neq 0,1} \sigma_{ij} \mathcal{T}_{ij} + E_A \mathcal{P}_0 + E_B \mathcal{P}_1 + V(\mathcal{T}_{01} + \mathcal{T}_{10}). \tag{2.14}$$

By simple partitioning of the space into a space spanned by 0 and 1 and the rest, we get

$$G_{00} = \frac{\beta_B G_{00}^{\text{eff}} - G_{01}^{\text{eff}}[(\sigma_0 - E_B)G_{10}^{\text{eff}} + \alpha]}{\beta_A \beta_B - [(\sigma_0 - E_A)G_{01}^{\text{eff}} + \alpha][(\sigma_0 - E_B)G_{10}^{\text{eff}} + \alpha]} \tag{2.15a}$$

$$G_{11} = \frac{\beta_A G_{00}^{\text{eff}} - G_{10}^{\text{eff}}[(\sigma_0 - E_A)G_{01}^{\text{eff}} + \alpha]}{\beta_A \beta_B - [(\sigma_0 - E_B)G_{10}^{\text{eff}} + \alpha][(\alpha_0 - E_A)G_{01}^{\text{eff}} + \alpha]} \tag{2.15b}$$

where G_{ij}^{eff} is the Green function for the effective medium, and

$$\begin{aligned} \alpha &= (\sigma_1 - V)G_{00}^{\text{eff}} \\ \beta_A &= 1 + (\sigma_0 - E_A)G_{00}^{\text{eff}} + (\sigma_1 - V)G_{10}^{\text{eff}} \\ \beta_B &= 1 + (\sigma_0 - E_B)G_{00}^{\text{eff}} + (\sigma_1 - V)G_{01}^{\text{eff}}. \end{aligned} \tag{2.15c}$$

The local density of states (LDOS) ρ_i on the ith site is then obtained as

$$\rho_i = -(1/\pi)\,\text{Im}(G_{ii}^{\text{eff}}) \qquad i = 0 \text{ or } 1.$$

2.3. Korringa–Kohn–Rostoker cluster coherent-potential approximation (KKR-CCPA)

In the KKR framework the alloy is modelled by a random array of muffin-tin potentials of A or B type. The on-shell matrix elements of single muffin-tin t-matrices are (Ehrenreich and Schwartz 1976, Gyorffy and Stocks 1979, Bansil 1987)

$$t_l^{A(B)}(\kappa) = -(1/\kappa)\, e^{i\delta_l} \sin \delta_l \tag{2.16}$$

where $\kappa = (|E|)^{1/2}$ and δ_l are phase shifts. The path operator matrices are given by

$$T_{ij} = \{[C - B(\kappa)]^{-1}\}_{ij} \tag{2.17}$$

where $C = t^{-1}$ and $B(\kappa)$ is the matrix of real-space structure function $B_{ij}(\kappa)$ (Ehrenreich and Schwartz 1976). We note that $B(\kappa)$ depends only on the lattice structure and does not contain any disorder while $C(\kappa)$ has a binary distribution. For a random binary alloy the random variable C can be written in terms of the random parameter n_i as

$$C_i = C_A n_i + C_B(1 - n_i)$$

where n_i is given by equation (2.1c). Also we define an operator D as

$$D = T^{-1} = C - B = \sum_i C_i \mathcal{P}_i - \sum_{i \neq j} \sum B_{ij} \mathcal{T}_{ij} = C_B + \delta C \sum_i \mathcal{P}_i n_i - \sum_{i \neq j} \sum B_{ij} \mathcal{T}_{ij}$$

and

$$\delta C = C_A - C_B.$$

A comparison of (2.17) and (2.1b) shows that T_{ij} is structurally similar to G_{ij} and hence the augmented-space formulation developed in section 2.1 for the tight-binding equations can be applied straightforwardly to derive the KKR-CCPA equations (Mookerjee 1987). The relationship between tight-binding and KKR formulations becomes clear if we note the following correspondences:

$$\begin{aligned} G &\leftrightarrow T \\ E &\leftrightarrow C \\ V &\leftrightarrow -B \\ H_I, H_{II} &\leftrightarrow D_I, D_{II}. \end{aligned} \tag{2.18}$$

The procedure for generating the CPA and CCPA by partitioning of the augmented space is identical to that described in section 2.1. By using (2.18), we get the KKR-CCPA equations as

$$\begin{aligned} C &= \bar{C} - W' Q'_{66} W' \\ \mathcal{B}_{01} &= B_{01} + W' Q'_{61} W' \\ \mathcal{B}_{10} &= B_{10} + W' Q'_{16} W'. \end{aligned} \tag{2.19}$$

Here

$$\begin{aligned}
\mathcal{B}_{ij} &= B_{ij} + b_{ij} \\
Q'_{66} &= R'^{-1}_6 \\
Q'_{16} &= R'^{-1}_1 \mathcal{V}'_{10} R'^{-1}_2 W' R'^{-1}_3 \mathcal{V}'_{01} R'^{-1}_4 W' R'^{-1}_5 \mathcal{V}'_{10} R'^{-1}_6 \\
Q'_{61} &= R'^{-1}_6 \mathcal{V}'_{01} R'^{-1}_5 W' R'^{-1}_4 \mathcal{V}'_{10} R'^{-1}_3 W' R'^{-1}_2 \mathcal{V}'_{01} R'^{-1}_1
\end{aligned} \tag{2.20}$$

with

$$\begin{aligned}
\mathcal{V}'_{01} &= B_{01} + \xi'_{01} \\
\mathcal{V}'_{10} &= B_{10} + \xi'_{10}
\end{aligned}$$

and

$$\begin{aligned}
R'_1 &= \bar{C} - \xi'_{00} \\
R'_2 &= \bar{C} - \xi'_{00} - \mathcal{V}'_{01} R'^{-1}_1 \mathcal{V}'_{10} \\
R'_3 &= \bar{C} - \xi'_{00} - W' R'^{-1}_2 W' \\
R'_4 &= \bar{C} - \xi'_{00} - \mathcal{V}'_{10} R'^{-1}_3 \mathcal{V}'_{01} \\
R'_5 &= \bar{C} - \xi'_{00} - W' R'^{-1}_4 W' \\
R'_6 &= \bar{C} - \xi'_{00} - \mathcal{V}'_{01} R'^{-1}_5 \mathcal{V}'_{10}
\end{aligned} \tag{2.21}$$

where

$$\bar{C} = xC_A + yC_B \qquad \tilde{C} = xC_B + yC_A \qquad W' = (xy)^{1/2}(C_A - C_B).$$

Also

$$\begin{aligned}
\xi'_{00} &= C - [T^{\text{eff}}_{00} - T^{\text{eff}}_{01}(T^{\text{eff}}_{00})^{-1} T^{\text{eff}}_{10}]^{-1} \\
\xi'_{01} &= -\mathcal{B}_{01} + [T^{\text{eff}}_{00} - T^{\text{eff}}_{01}(T^{\text{eff}}_{00})^{-1} T^{\text{eff}}_{10}]^{-1} T^{\text{eff}}_{01}(T^{\text{eff}}_{00})^{-1} \\
\xi'_{10} &= -\mathcal{B}_{10} + (T^{\text{eff}}_{00})^{-1} T^{\text{eff}}_{10} [T^{\text{eff}}_{00} - T^{\text{eff}}_{01}(T^{\text{eff}}_{00})^{-1} T^{\text{eff}}_{10}]^{-1}.
\end{aligned} \tag{2.22}$$

Now the average electronic density of states for the alloy can be calculated by the formula (Ehrenreich and Schwartz 1976)

$$\delta\rho(E) = \rho_{\text{eff}}(E) - \rho_0(E) = \frac{-1}{N\pi} \operatorname{Im} \operatorname{Tr} \left(\left\langle T \frac{\mathrm{d}C}{\mathrm{d}E} \right\rangle - \langle T \rangle \frac{\mathrm{d}B_q}{\mathrm{d}E} \right) \tag{2.23}$$

where $\rho_0(E)$ is the free-electron DOS, $\rho_{\text{eff}}(E)$ is the DOS for the effective medium, N is the total number of unit cells in the solid and B_q is the Fourier transform of B_{ij}. The configuration averages in equation (2.23) can be calculated using the augmented-space formalism as shown in section 3.1.

3. Application of the cluster coherent-potential approximation

3.1. The s phase shift semicircular model

We shall illustrate our KKR-CCPA formalism by applying it to a simple model. This will also bring us in contact with the single-site muffin-tin KKR-CPA work of Soven (1970). As in that work, we shall assume that only the s phase shift dominates, so that B, t and T

become scalars in angular-momentum space. For this model, like Soven (1970), we shall assume that the phase shift has resonance behaviour and that the cotangent of phase shift is given by

$$c_{A(B)} = (E_{A(B)} - E)/\Gamma_{A(B)} \tag{3.1}$$

where $E_{A(B)}$ is the resonant energy and $\Gamma_{A(B)}$ is the resonance half-width.

In order to simplify the problem further, we assume that the structure function (Soven 1970)

$$\tilde{B}_q = (B_q/\kappa) - i \tag{3.2}$$

has no explicit dependence on energy. Here $B_q(\kappa)$ is the Fourier transform of B_{ij}. From (2.16) we get

$$C(\kappa) = t^{-1}(\kappa) = -\kappa \cot \delta_0 + i = -\kappa c + i \tag{3.3}$$

where c is given by equation (3.1).

The path operator

$$\begin{aligned} T_{ij} &= \frac{1}{N}\sum_q \exp(-i\boldsymbol{q}\cdot\boldsymbol{R}_{ij})\frac{1}{c - B_q} \\ T_{00} &= -\frac{1}{\kappa N}\sum_q (c + \tilde{B}_q)^{-1} = -\frac{1}{\kappa}\int (c+b)^{-1} f^0(b)\,\mathrm{d}b \end{aligned} \tag{3.4}$$

where $f^0(b)$ is a distribution function given by

$$f^0(b) = \frac{1}{N}\sum_q \delta(b - \tilde{B}_q). \tag{3.5}$$

We choose $f^0(b)$ (Soven 1970) as

$$f^0(b) = \begin{cases} (2/\pi)(1 - b^2)^{1/2} & |b| \leqslant 1 \\ 0 & |b| > 1. \end{cases} \tag{3.6}$$

Then

$$T_{00} = -(1/\kappa)g_{00}$$

where

$$g_{00} = 2[c + (c^2 - 1)^{1/2}]. \tag{3.7}$$

Similarly,

$$T_{01} = T_{10} = -\frac{1}{\kappa}\int f'(b)(c+b)^{-1}\,\mathrm{d}b \tag{3.8a}$$

where distribution function $f'(b)$ is defined as

$$f'(b) = \frac{1}{N}\sum_{q} \exp(-\mathrm{i}\boldsymbol{q}\cdot\boldsymbol{R}_{01})\,\delta(b-\tilde{B}_q). \tag{3.8b}$$

We choose $f'(b)$ such that

$$f'(b) = \begin{cases} = -(\lambda/\pi)(1-b^2)^{1/2}b & |b| \leqslant 1 \\ = 0 & |b| > 1 \end{cases} \tag{3.9}$$

where λ is a constant. The validity of this choice will be discussed in section 3.3. Hence

$$T_{01} = T_{10} = -\frac{1}{\kappa}\int_{-1}^{+1}\left(\frac{-\lambda}{\pi}\right)(1-b^2)^{1/2}(c+b)^{-1}b\,\mathrm{d}b = -\frac{1}{\kappa}g_{01}$$

where

$$g_{01} = (\lambda/8)(g_{00})^2. \tag{3.10a}$$

From equation (3.8*b*) we get

$$\tilde{B}_{01} = \int f'(b)b\,\mathrm{d}b = -\lambda/8. \tag{3.10b}$$

Taking the Fourier transform of (3.2) we get

$$B_{01} = B_{10} = \kappa\tilde{B}_{01} = -\kappa\lambda/8.$$

From equation (2.20) we get

$$\mathcal{B}_{01} = \mathcal{B}_{10} = B_{01} + b_{01}$$

where

$$b_{01} = b_{10} = \kappa\beta_{01}. \tag{3.11}$$

The Fourier transform of (3.11) gives us

$$\mathcal{B}_q = B_q + b_q$$

and

$$b_q(\kappa) = \sum_{j\neq 0} b_{0j}\exp(\mathrm{i}\boldsymbol{q}\cdot\boldsymbol{R}_{0j}) = b_{01}\exp(\mathrm{i}\boldsymbol{q}\cdot\boldsymbol{R}_{01}).$$

The diagonal elements of the path operator within the CCPA are given as

$$T_{00}^{\mathrm{eff}} = -\frac{1}{\kappa N}\sum_{q}(c+\tilde{B}_q)^{-1}\left(1+\frac{\beta_{01}\exp(\mathrm{i}\boldsymbol{q}\cdot\boldsymbol{R}_{01})}{c+\tilde{B}_q}\right)^{-1}.$$

Expanding in a Taylor series near $\beta_{01} = 0$ and retaining only the first-order term we get

$$T_{00}^{\mathrm{eff}} = -(1/\kappa)g_{00}^{\mathrm{eff}}$$

where

$$g_{00}^{\text{eff}} = g_{00} + \lambda\beta_{01}\left(2c + \frac{2c^2 - 1}{(c^2 - 1)^{1/2}}\right). \tag{3.12}$$

The off-diagonal elements of the path operator are given by

$$T_{01}^{\text{eff}} = -\frac{1}{\kappa N}\sum_{q} \exp(-\mathrm{i}\boldsymbol{q}\cdot\boldsymbol{R}_{01})(c + \tilde{B}_q)^{-1}\left(1 + \frac{\beta_{01}\exp(\mathrm{i}\boldsymbol{q}\cdot\boldsymbol{R}_{01})}{c + \tilde{B}_q}\right)^{-1}$$

which reduces to

$$T_{01}^{\text{eff}} = T_{10}^{\text{eff}} = -(1/\kappa)g_{01}^{\text{eff}}$$

where

$$g_{01}^{\text{eff}} = g_{01} + 2\beta_{01}[1 + c/(c^2 - 1)^{1/2}]. \tag{3.13}$$

Note that the form of the function g_{01}^{eff} retains its *herglotz* properties even after this additional approximation.

Finally the change in DOS per atom is given by equation (2.23), which is

$$\delta\rho(E) = -\frac{\text{Im}}{\pi}\left(\left\langle T_{00}\frac{\mathrm{d}C}{\mathrm{d}E}\right\rangle - \frac{1}{N}\sum_{q}(C^{\text{eff}} - B_q - b_q)^{-1}\frac{\mathrm{d}(B_q + b_q)}{\mathrm{d}E}\right) \tag{3.14}$$

where

$$\left\langle T_{00}\frac{\mathrm{d}C}{\mathrm{d}E}\right\rangle = T_{00}^{\text{eff}}U^{\text{eff}}$$

$$U^{\text{eff}} = \bar{U} + \frac{C^{\text{eff}} - \bar{C}}{C_{\text{A}} - C_{\text{B}}}(U_{\text{A}} - U_{\text{B}})$$

$$U = \mathrm{d}C/\mathrm{d}E \qquad C^{\text{eff}} = -\kappa c + i.$$

We get the formula for the change in DOS as

$$\delta\rho(E) = \frac{\text{Im}}{\pi}\left\{g_{00}^{\text{eff}}\left[\frac{x}{\Gamma_{\text{A}}} + \frac{y}{\Gamma_{\text{B}}} + \frac{c - \bar{c}}{c_{\text{A}} - c_{\text{B}}}\left(\frac{1}{\Gamma_{\text{A}}} - \frac{1}{\Gamma_{\text{B}}}\right)\right]\right\} \tag{3.15}$$

where $\bar{c} = xc_{\text{A}} + yc_{\text{B}}$ and c is the cotangent of the phase shift for the effective medium.

3.2. *The Bethe lattice model*

Bethe lattices have no closed loops and are completely characterised by their number of nearest neighbours Z or connectivity $K = Z - 1$. For the tight-binding Hamiltonian on the Bethe lattice the Green functions for a perfect system can be calculated exactly by a renormalised perturbation expansion (Economou 1979) and are given by

$$\begin{aligned} G_{00} &= \frac{2K}{(K-1)(E - E_0) + (K+1)[(E - E_0)^2 - 4KV^2]^{1/2}} \\ G_{01} &= G_{10} = G_{00}\left(\frac{2V}{(E - E_0) + [(E - E_0)^2 - 4KV^2]^{1/2}}\right) \end{aligned} \tag{3.16}$$

where E_0 and V are the diagonal and off-diagonal elements of the nearest-neighbour Hamiltonian. We take $V = 0.5/K^{1/2}$, which gives unit half band-width. For an alloy A_xB_y

we take the site energies E_0 as $E_A = \delta/2$ and $E_B = -\delta/2$, where δ is a band separation parameter. For the CPA medium, (3.16) reduces to

$$G_{00} = \frac{2K}{(K-1)(E-\sigma_0) + (K+1)[(E-\sigma_0)^2 - 4KV^2]^{1/2}}$$
$$G_{01} = G_{10} = G_{00}\left(\frac{2V}{(E-\sigma_0) + [(E-\sigma_0)^2 - 4KV^2]^{1/2}}\right) \tag{3.17}$$

where σ_0 is the diagonal element of the effective Hamiltonian within the CPA. For $K \gg 1$, equations (3.17) reduce to the Green function of the semicircular model (Velicky *et al* 1968) as

$$G_{00} = 2\{(E-\sigma_0) - [(E-\sigma_0)^2 - 1]^{1/2}\}$$
$$G_{01} = G_{10} = (0.5/K^{1/2})(G_{00})^2. \tag{3.18}$$

The Green functions within the CCPA can be obtained from (3.17) by replacing V by σ_1, where σ_1 is the off-diagonal element of the effective Hamiltonian.

3.3. Comparison of KKR-CCPA and TB-CCPA equations

In this section, we compare the KKR-CCPA equations for the s phase shift semicircular model of unit resonance half-width with the TB-CCPA equations for the semicircular model of unit half band-width. Therefore, we have calculated the values of Green functions for tight-binding semicircular model with the help of distribution functions. The Green function within the CPA is given by (Ehrenreich and Schwartz 1976)

$$G_{ij} = \frac{1}{N}\sum_{\boldsymbol{q}} \frac{\exp(-i\boldsymbol{q}\cdot\boldsymbol{R}_{ij})}{E - \sigma_0 - S_{\boldsymbol{q}}} \tag{3.19}$$

where

$$S_{\boldsymbol{q}} = \frac{1}{N}\sum\sum_{i\neq j} \exp(i\boldsymbol{q}\cdot\boldsymbol{R}_{ij})V_{ij}.$$

With the help of distribution functions $f^0(b)$ and $f'(b)$ as defined in (3.6) and (3.9), we get

$$G_{00} = -\int f^0(b)(c'+b)^{-1}\,db = -2[c' + (c'^2 - 1)^{1/2}] \tag{3.20}$$

$$G_{01} = G_{10} = \int f'(b)(c'+b)^{-1}\,db = -(\lambda/8)(G_{00})^2 \tag{3.21}$$

where

$$c' = \sigma_0 - E.$$

These equations for G_{00} and G_{01} are analogous to equations (3.18), which are exact and are derived by taking the large-K limit of the Bethe lattice model. Since T_{ij} in equation (3.4) and G_{ij} in equation (3.19) are structurally similar, we expect T_{00} and T_{01} in equations (3.7) and (3.10*a*) respectively to have the form of equations (3.20) and

(3.21). This is exactly what we get by using the distribution functions $f^0(b)$ and $f'(b)$. Therefore, we are justified in using these distribution functions. We also get

$$V_{01} = V_{10} = \int f'(b) b \, \mathrm{d}b = -\lambda/8. \tag{3.22}$$

The Green function for the effective medium is given by

$$G_{ij}^{\mathrm{eff}} = \frac{1}{N} \sum_{q} \frac{\exp(-\mathrm{i}\boldsymbol{q} \cdot \boldsymbol{R}_{ij})}{E - \sigma_0 - \tilde{S}_q} \tag{3.23a}$$

where

$$\tilde{S}_q = S_q + s_q \qquad s_q = v_{01} \exp(\mathrm{i}\boldsymbol{q} \cdot \boldsymbol{R}_{ij}) \qquad v_{ij} = \sigma_{ij} - V_{ij}. \tag{3.23b}$$

By using the distribution functions $f^0(b)$ and $f'(b)$, we have calculated the diagonal and off-diagonal elements of G^{eff} as

$$G_{00}^{\mathrm{eff}} = G_{00} - \lambda v_{01} \left(2c' + \frac{2c'^2 - 1}{(c'^2 - 1)^{1/2}} \right)$$

$$G_{01}^{\mathrm{eff}} = G_{01} - 2v_{01} \left(1 + \frac{c'}{(c'^2 - 1)^{1/2}} \right).$$

Now for convenience, we define a new set of KKR variables as follows:

$$\begin{aligned}
&\beta'_{01} = \beta_{01}/\kappa && j_0 = \xi'_{00}/\kappa + i \\
&j_1 = \xi'_{01}/\kappa && v' = \mathcal{V}'_{01}/\kappa \\
&r_1 = R'_1/\kappa && r_2 = R'_2/\kappa \\
&r_3 = R'_3/\kappa && r_4 = R'_4/\kappa \\
&r_5 = R'_5/\kappa && r_6 = R'_6/\kappa \\
&Q''_{61} = \kappa Q'_{61} && Q''_{61} = Q''_{16} \\
&w = W'/\kappa.
\end{aligned} \tag{3.24}$$

By using these variables, the KKR-CCPA equations are compared with TB-CCPA equations in table 1. It is clear that there is a one-to-one correspondence between them.

4. Results and discussion

For convenience, we shall first present the calculations using the tight-binding method for the Bethe lattice model with $K = 2$. Figure 1 shows the CPA and CCPA DOS for $\delta = 1$ in the low-concentration regime. We note that there is not much difference in the majority band between the CPA and CCPA, in contrast to considerable difference in the impurity band. Two sub-bands appear in the CCPA as compared to one in the CPA. These two sub-bands arise because of correlated scattering from the clusters of two impurities embedded in the effective medium. In the low-concentration limit ($x \ll 1$), the impurity pair in the alloy is most likely to be of AA type. The energy levels for the AA impurity pair embedded in pure B are at energies 0.53 and 1.04, as shown by the full arrows in figure 1. These two levels are close to the shoulder in the CCPA DOS at about $E = 0.6$ and

Table 1. Comparison between KKR-CCPA and TB-CCPA equations.

KKR-CCPA equations	TB-CCPA equations
$\beta'_{01} = -\lambda/8$	$V_{01} = -\lambda/8$
$w = (xy)^{1/2}(E_A - E_B)$	$W = (xy)^{1/2}(E_A - E_B)$
$\bar{c} = xE_A + yE_B - E$	$\bar{E} = xE_A + yE_B$
$\tilde{c} = yE_A + xE_B - E$	$\tilde{E} = yE_A + xE_B$
$g_{00}^{\text{eff}} = 2[c + (c^2-1)^{1/2}] + \lambda\beta_{01}\left(2c + \frac{2c^2-1}{(c^2-1)^{1/2}}\right)$	$G_{00}^{\text{eff}} = -2[c' + (c'^2-1)^{1/2}] - \lambda\upsilon_{01}\left(2c' + \frac{2c'^2-1}{(c'^2-1)^{1/2}}\right)$
$g_{01}^{\text{eff}} = (\lambda/2)[2c^2 - 1 + 2c(c^2-1)^{1/2}] + 2\beta_{01}\left(1 + \frac{c}{(c^2-1)^{1/2}}\right)$	$G_{01}^{\text{eff}} = -(\lambda/2)[2c'^2 - 1 + 2c'(c'^2-1)^{1/2}] - 2\upsilon_{01}\left(1 + \frac{c'}{(c'^2-1)^{1/2}}\right)$
$j_0 = -c + g_{00}^{\text{eff}}[(g_{00}^{\text{eff}})^2 - (g_{01}^{\text{eff}})^2]^{-1}$	$\xi_{00} = -c' - G_{00}^{\text{eff}}[(G_{00}^{\text{eff}})^2 - (G_{01}^{\text{eff}})^2]^{-1}$
$j_1 = -\mathcal{B}'_{01} + g_{01}^{\text{eff}}[(g_{00}^{\text{eff}})^2 - (g_{01}^{\text{eff}})^2]^{-1}$	$\xi_{01} = -\sigma_1 - G_{01}^{\text{eff}}[(G_{00}^{\text{eff}})^2 - (G_{01}^{\text{eff}})^2]^{-1}$
$v' = \beta'_{01} + j_1$	$\mathcal{V}_1 = V_{01} + \xi_{01}$
$r_1 = -\tilde{c} - j_0$	$R_1 = E - \tilde{E} - \xi_{00}$
$r_2 = -\bar{c} - j_0 - v'^2 r_1^{-1}$	$R_2 = E - \bar{E} - \xi_{00} - \mathcal{V}_1^2 R_1^{-1}$
$r_3 = -\tilde{c} - j_0 - w^2 r_2^{-1}$	$R_3 = E - \tilde{E} - \xi_{00} - W^2 R_2^{-1}$
$r_4 = -\tilde{c} - j_0 - v'^2 r_3^{-1}$	$R_4 = E - \tilde{E} - \xi_{00} - \mathcal{V}_1^2 R_3^{-1}$
$r_5 = -\bar{c} - j_0 - w^2 r_4^{-1}$	$R_5 = E - \bar{E} - \xi_{00} - W^2 R_4^{-1}$
$r_6 = -\tilde{c} - j_0 - v'^2 r_5^{-1}$	$R_6 = E - \tilde{E} - \xi_{00} - \mathcal{V}_1^2 R_5^{-1}$
$Q''_{61} = w^2 v'^3 / r_1 r_2 r_3 r_4 r_5 r_6$	$Q_{61} = W^2 \mathcal{V}_1^3 / R_1 R_2 R_3 R_4 R_5 R_6$
$c = \bar{c} + w^2/r_6$	$\sigma_0 = \bar{E} + W^2/R_6$
$\mathcal{B}'_{01} = \beta'_{01} + w^2 Q''_{61}$	$\sigma_1 = V_{01} + W^2 Q_{61}$
$\delta\rho(E) = (1/\pi)\,\text{Im}(g_{00}^{\text{eff}})$	$\rho(E) = -(1/\pi)\,\text{Im}(G_{00}^{\text{eff}})$

the peak at $E = 1.0$ respectively. The peak at about $E = 0.8$ in the CCPA DOS arises due to the single A impurity level, which is at $E = 0.83$ and about which the CPA impurity band is centred. Thus, the structures in the CCPA minority-band DOS are accounted for by the examination of impurity levels.

Figure 2(*a*) shows the CPA and CCPA DOS for $\delta = 1$ for a concentrated alloy ($x = 0.5$). We note that although the CPA DOS is smooth, the CCPA DOS has two peaks. We explain this on the basis of clusters of two atoms embedded in the effective medium. Unlike the low-concentration limit, the probabilities of AA, AB, BA and BB pairs are identical.

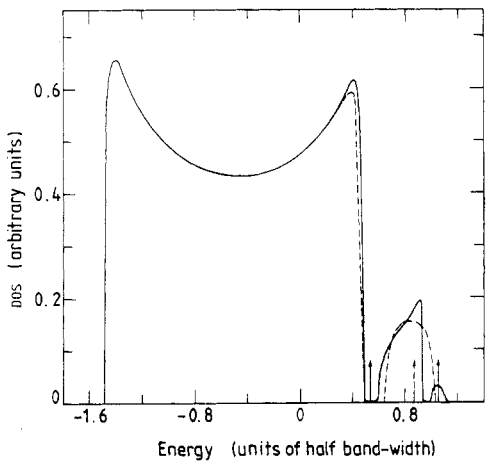

Figure 1. The averaged density of states using the CPA (broken curve) and the CCPA (full curve) for the parameters $K = 2$, $\delta = 1$ and $x = 0.05$. Broken and full arrows indicate the positions of the single-impurity and two-impurities levels in a pure B medium. The energy is in units of half band-width.

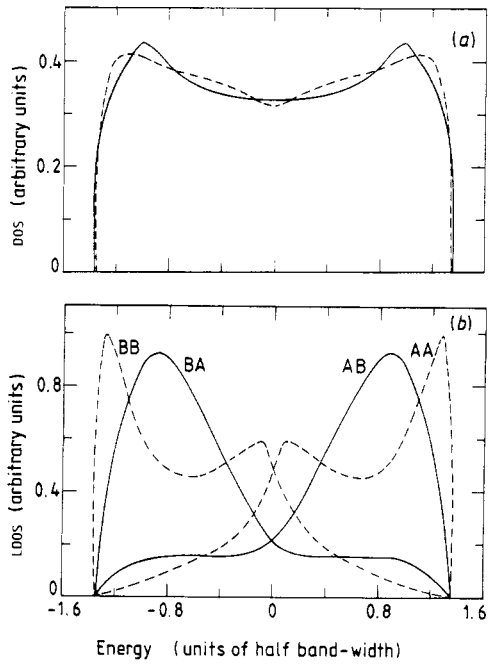

Figure 2. (*a*) The averaged density of states using the CPA (broken curve) and the CCPA (full curve) for parameters $K = 2$, $\delta = 1$ and $x = 0.5$. (*b*) Local density of states for two-impurities pairs embedded in the CPA medium for the same parameters. Full curves correspond to BA and AB pairs while broken curves correspond to BB and AA pairs.

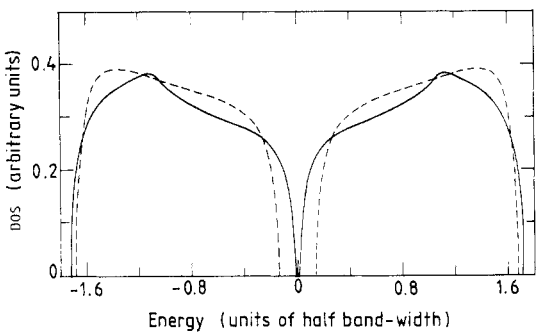

Figure 3. The averaged density of states using the CPA (broken curve) and the CCPA (full curve) for parameters $K = 2$, $\delta = 1.7$ and $x = 0.5$.

The peaks in CCPA around $E = -1.0$ and 1.0 appear approximately at energies close to the LDOS peaks corresponding to BA and AB pairs embedded in the CPA medium as shown in figure 2(*b*). The LDOS peaks corresponding to AA and BB pairs appear near the edges of the CCPA DOS. This indicates that the extra peaks arising in the CCPA DOS are due to the correlated scattering from the impurity clusters in the effective medium.

Figure 3 shows the DOS for $\delta = 1.7$ and $x = 0.5$. We note that the critical value of δ for band separation in the CCPA is 1.7 while in the CPA it is 1.3. This implies that in the CCPA the bands are less likely to be separated.

The results for the Bethe lattice model with $K = 10$ are shown in figures 4, 5 and 6. In figure 4 we show the CPA and CCPA DOS for $\delta = 1$ in the dilute limit ($x = 0.05$). There is no difference in the CPA and CCPA DOS in the majority band. The CCPA minority-band DOS has two peaks at about $E = 0.6$ and 0.85, in contrast to a very smooth CPA minority band. The two peaks in the CCPA DOS are well accounted for by the energy levels of AA impurity pairs, which are at $E = 0.64$ and 0.87 respectively.

Figure 5(*a*) shows the DOS curves for $\delta = 1$ in the concentrated limit ($x = 0.5$). We

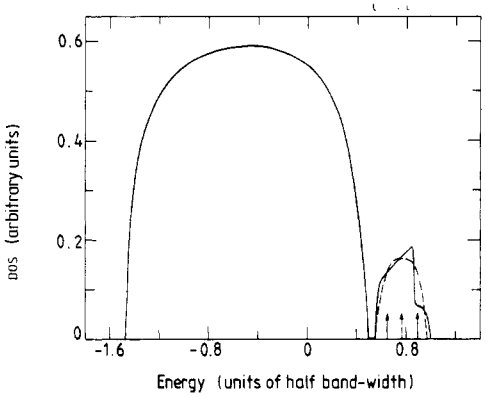

Figure 4. The averaged density of states using the CPA (broken curve) and the CCPA (full curve) for parameters $K = 10$, $\delta = 1$ and $x = 0.05$. The broken and full arrows indicate the positions of the single-impurity and two-impurities levels in a pure B medium.

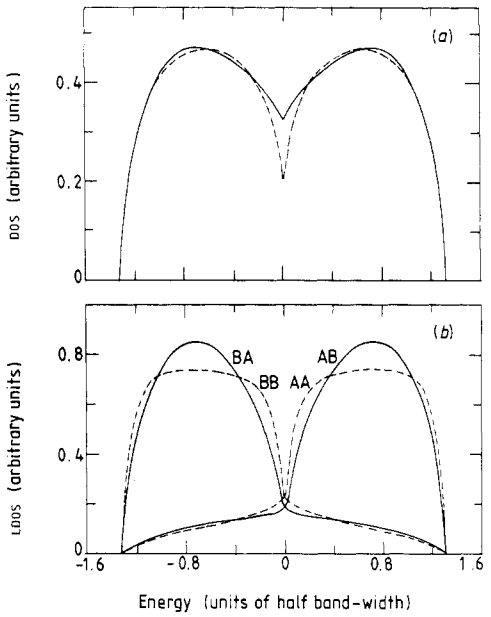

Figure 5. (*a*) The averaged density of states using the CPA (broken curve) and the CCPA (full curve) for parameters $K = 10$, $\delta = 1$ and $x = 0.5$. (*b*) Local density of states for two-impurities pairs embedded in the CPA medium for the same parameters. Full curves correspond to BA and AB pairs while broken curves correspond to BB and AA pairs.

note that both the CPA as well as the CCPA DOS are smooth. This arises for the following reasons: (i) the LDOS for the impurity pairs, as shown in figure 5(*b*), are smooth as compared to $K = 2$; (ii) the LDOS peaks for (BA, AB) and (AB, AA) pairs are at about the same energies.

Figure 6 shows the DOS for $\delta = 1.4$ and $x = 0.5$. This again shows that the critical value of δ in the CCPA is greater than that in the CPA. It is 1.4 in the CCPA whereas it is 1.2 in the CPA.

A contrast between $K = 2$ and $K = 10$ cases is worth noting. In the dilute limit, the minority band for $K = 2$ (figure 1) breaks up into two sub-bands while for $K = 10$ (figure 4) we have only one impurity band with some structure. The separation between the two impurity levels for the $K = 2$ case is much larger than that for $K = 10$. The difference is due to the different values of hopping parameter $V = 0.5/K^{1/2}$ in the two cases. For the $K = 10$ case it is much smaller compared to that for $K = 2$. Thus in the concentrated limit, there is an appreciable difference in the CPA and CCPA DOS for $K = 2$ compared to $K = 10$. The difference between the CPA and CCPA DOS decreases as K increases and eventually reduces to zero when K is very large ($\simeq 100$). Note that, in this limit, our model reduces to the semicircular model (Velicky *et al* 1968) as shown in section 3.2.

Now we present the KKR-CCPA results for the s phase shift semicircular model. We have calculated the change in density of states (δDOS) with respect to the free-electron gas within the CPA and CCPA. We have found that, for the small λ, there is negligible

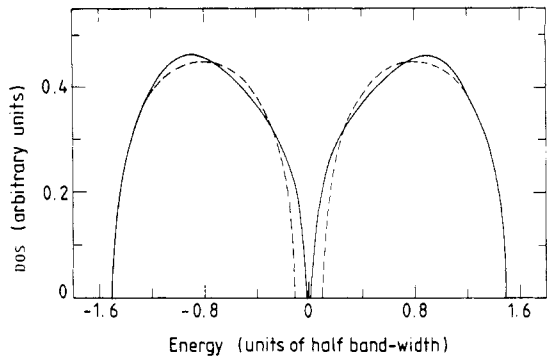

Figure 6. The averaged density of states using the CPA (broken curve) and the CCPA (full curve) for parameters $K = 10$, $\delta = 1.4$ and $x = 0.5$.

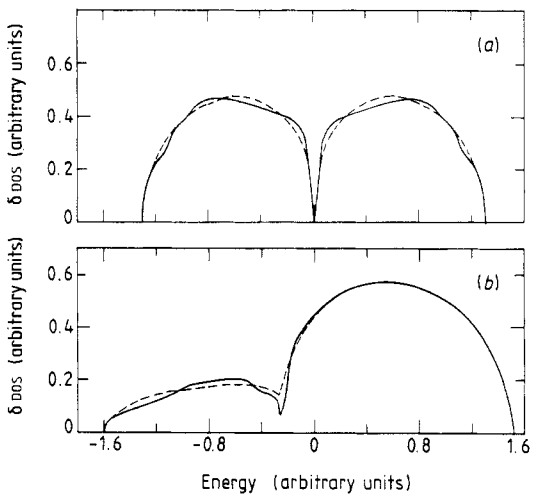

Figure 7. (*a*) The change in averaged density of states per atom using the KKR-CPA (broken curve) and the KKR-CCPA (full curve) for the parameters $E_A = -E_B = 0.5, \Gamma_A = 1, \Gamma_B = 1, \lambda = 2.5$ and $x = 0.5$. The energy is in arbitrary units. (*b*) Same as in (*a*) but with parameters $E_A = -E_B = 0.5, \Gamma_A = 1, \Gamma_B = 2, \lambda = 2.5$ and $x = 0.8$.

difference in δDOS between the CPA and CCPA, as was mentioned above for the Bethe lattice model with large K. This is because for large K (or small λ), CCPA equations for both models have one-to-one correspondence. But for large λ there is a visible difference between δDOS in the CPA and CCPA as can be seen in figures 7(*a*) and (*b*). Figure 7(*a*) shows the KKR-CPA and KKR-CCPA δDOS for the same resonance half-widths ($\Gamma_A = \Gamma_B = 1$), while figure 7(*b*) is for different half-widths ($\Gamma_A = 1, \Gamma_B = 2$). Note that these results, in general, are also valid for the tight-binding semicircular model, as is evident from table 1.

As in the tight-binding case, to understand the structure in the KKR-CCPA DOS, we have to solve the two-impurities problem. This requires knowledge of the impurity wavefunctions (Faulkner and Stocks 1980), which are not available for the s phase shift model. However, since we have already shown a one-to-one correspondence between the KKR-CCPA and the TB-CCPA equations, we expect that the main features of the TB model will be reflected in the KKR model, and hence the structure in figure 7 can be related to the correlated scattering from clusters of atoms.

5. Conclusions

We have applied the KKR-CCPA formulation to the s phase shift semicircular model, which has an analogue in the tight-binding framework. A one-to-one correspondence has been established between the KKR-CCPA equations for this model and the TB-CCPA equations for the analogous semicircular model. In the course of this analysis, we were also able to refine the TB-CCPA method such that various quantities, which have so far been calculated approximately, are calculated *exactly*. This TB-CCPA formulation was then applied to the Bethe lattice model. We found that the difference in the CPA and CCPA DOS is appreciable only when the number of nearest neighbours Z is small and decreases as Z increases. Also, in the CPA the minority band is smooth whereas in the CCPA it gains structure. The structure in the CCPA DOS is seen at energies close to the impurity levels. This clearly indicates that the structure appears due to the correlated scattering from the clusters embedded in an effective medium. For a large value of Z, there is little difference in the CPA and CCPA DOS for this model and the s phase shift semicircular model. This is expected because of their equivalence in this limit.

Acknowledgment

This work was supported by the Department of Science and Technology, New Delhi, India.

References

Banhart J, Pfeiler W and Voitlander J 1988 *Phys. Rev.* B **37** 6027
Bansil A 1987 *Electronic Band Structure and its Applications* ed M Yussouff (Berlin: Springer) p 273
Economou E N 1979 *Green's Functions in Quantum Mechanics* (Berlin: Springer) p 90
Ehrenreich H and Schwartz L M 1976 *Solid State Phys.* **31** 149
Faulkner J S and Stocks G M 1980 *Phys. Rev.* B **21** 3222
Gonis A, Stocks G M, Butler W H and Winter H 1984 *Phys. Rev.* B **29** 555
Gray L J and Kaplan T 1976a *Phys. Rev.* B **14** 3462
—— 1976b *J. Phys. C: Solid State Phys.* **9** L303, L483
Gyorffy B L and Stocks G M 1979 *Electrons in Disordered Metals and at Metallic Surfaces* ed P Phariseau, B L Gyorffy and L Scheire (New York: Plenum) p 89
Kumar V, Mookerjee A and Srivastava V K 1982 *J. Phys. C: Solid State Phys.* **15** 1939
Mills R and Ratanavararaksa P 1978 *Phys. Rev.* B **18** 5291
Mookerjee A 1973 *J. Phys. C: Solid State Phys.* **6** L205, 1340
—— 1987 *J. Phys. F: Met. Phys.* **17** 1511
Razee S S A, Rajput S S, Prasad R and Mookerjee A 1990 unpublished
Soven P 1970 *Phys. Rev.* B **2** 4715
Stefanou N, Zeller R and Dederichs P H 1987 *Solid State Commun.* **62** 735
Thakur P K, Mookerjee A and Singh V A 1987 *J. Phys. C: Solid State Phys.* **17** 1523
Velicky B, Kirkpatrick S and Ehrenreich H 1968 *Phys. Rev.* **175** 747
Wright H, Weightman P, Andrews P T, Folkerts W, Flipse C F J, Sawatzky G A, Norman D and Padmore H 1987 *Phys. Rev.* B **35** 519